Boulder and fine sediment transport and deposition by the 2004 tsunami in Lhok Nga (western Banda Aceh, Sumatra, Indonesia): A coupled offshore–onshore model

Article *in* Marine Geology · January 2010

DOI: 10.1016/j.margeo.2009.10.011

CITATIONS
170

READS
155

7 authors, including:

Raphaël Paris
Université Clermont Auvergne
178 PUBLICATIONS **3,023** CITATIONS
SEE PROFILE

Jérôme Fournier
French National Centre for Scientific Research
236 PUBLICATIONS **1,149** CITATIONS
SEE PROFILE

Emmanuel Poizot
Conservatoire National des Arts et Métiers
40 PUBLICATIONS **519** CITATIONS
SEE PROFILE

Samuel Etienne
Ecole Pratique des Hautes Etudes
158 PUBLICATIONS **1,326** CITATIONS
SEE PROFILE

Marine Geology 268 (2010) 43–54

Contents lists available at ScienceDirect

Marine Geology

journal homepage: www.elsevier.com/locate/margeo

Boulder and fine sediment transport and deposition by the 2004 tsunami in Lhok Nga (western Banda Aceh, Sumatra, Indonesia): A coupled offshore–onshore model

Raphaël Paris [a,*], Jérôme Fournier [b], Emmanuel Poizot [c], Samuel Etienne [a,d], Julie Morin [e], Franck Lavigne [f], Patrick Wassmer [f,g]

[a] GEOLAB UMR 6042 CNRS – UBP, Clermont-Ferrand, France
[b] BOREA UMR 7208 CNRS – MNHN, Dinard, France
[c] CNAM – Intechmer, Cherbourg, France
[d] Université de la Polynésie Française, Tahiti, French Polynesia
[e] LGSR, Université de La Réunion, St Denis, France
[f] Laboratoire de Géographie Physique UMR 8591 CNRS, Meudon, France
[g] Faculté de Géographie et d'Aménagement, Université de Strasbourg, France

ARTICLE INFO

Article history:
Received 17 March 2009
Received in revised form 28 September 2009
Accepted 15 October 2009
Available online 24 October 2009

Keywords:
tsunami deposits
boulders
sediment transport modelling
side-scan sonar
Sumatra
Indonesia

ABSTRACT

Estimating the magnitude of a past tsunami from its deposits is one of the major topics to be developed in future studies on tsunami hazard assessment. Main limitations are (1) the great variability of tsunami sandy sheets deposited on land (the sediment source and the topography controlling many aspects of the deposition), (2) the preservation of these soft sediments, and (3) the controversial interpretations of coastal boulder accumulations. In this paper, we investigate sediment transport and deposition during the December 26, 2004 tsunami inflow and outflow in the Lhok Nga Bay, located 10 km west of the city of Banda Aceh (northwest Sumatra, Indonesia). Side-scan sonar data of the near shore area are used to study the morphometry and distribution of boulders offshore. Entrainment of finer sediments offshore is inferred by estimating the movable grain sizes based upon the simulated current velocities of the tsunami waves. Results demonstrate that the tsunami waves raised the bed shear velocities to levels above critical values for the entrainment of coarse sands on the continental shelf. Most of the sediments deposited on land came from offshore, from fine sands to coral boulders. With very high values of u_* (>30 cm/s), the outflow (backwash) reworked and re-deposited large volume of sediments offshore. All rocky outcrops offshore were affected by the tsunami (down to 25 m deep). The fraction of boulders transported from offshore and deposited inland represents only 7% of the total number of boulders moved during the tsunami. Characteristics of the boulders can help to estimate flow velocities required for detaching them, and their imbrication (if any) to infer flow directions. However, calculations of flow depth and transport distance do not provide convincing results. Future studies coupling offshore–onshore mapping of boulder accumulations with reconstitutions of the morphological history (sea-level variations, coastal sediment discharge and landform evolution) may allow distinguishing storms and tsunami deposits.

1. Introduction

Despite considerable progress over the last fifteen years, we cannot yet conclusively deduce the magnitude (or "size") of past tsunamis after their deposits. As pointed out by Huntington et al. (2007), "inverse models of flow from tsunami deposits and forward models of deposits from flow are relatively new and still under development" (e.g. Jaffe and Gelfenbaum, 2007; Noda et al., 2007; Weiss, 2008; Pritchard and Dickinson, 2008). Developing such quantitative tools requires a better understanding and modelling of sediment transport and deposition by tsunamis of distinct magnitudes. Jaffe and Gelfenbaum (2007) proposed a model for calculating tsunami flow speed from the thickness and grain size of tsunami sandy deposits. Nevertheless, the sediment source and the topography control many aspects of the deposition inland: thickest deposits in the topographic lows, great spatial variations in thickness and upper laminated texture when the sedimentation was limited by steep slopes, very poor sorting and landward coarsening at the wave breaking line, multimodal grain-size distributions reflecting different sources of sediments (e.g. Nanayama and Shigeno, 2006; Paris et al., 2007; Choowong et al., 2008a,b).

A suite of diagnostic characteristics allows palaeo-tsunami deposits to be identified: they are locally extensive and generally finer inland and upwards, distinct upper and lower sub-units can be

* Corresponding author.
E-mail address: raparis@univ-bpclermont.fr (R. Paris).

0025-3227/$ – see front matter © 2009 Elsevier B.V. All rights reserved.
doi:10.1016/j.margeo.2009.10.011

identified, the lower contact is unconformable or erosional, the clast size varies from boulders to fine silt, there are fossil-rich sub-units (coral, shells), rip-up clasts of reworked material can be found (e.g. soil, roots, wood, debris), clasts fabrics and laminasets may indicate landward, seaward and oscillatory paleocurrents. These criteria have been confirmed and discussed through recent research on the December 26, 2004 tsunami deposits in Indonesia, Thailand, Sri Lanka and India (e.g. Bahlburg and Weiss, 2006; Goff et al., 2006a; Moore et al., 2006; Singarasubramanian et al., 2006; Szczucinski et al., 2006; Hori et al., 2007; Paris et al., 2007; Srinivasalu et al., 2007; Choowong et al., 2008a,b; Morton et al., 2008). Tsunami sandy deposits analysed by these authors for the same event but in different areas may display similar grain-size trends and thickness, even if flow depth and velocities were completely different.

Furthermore, most of the trench-scale (m) criteria presented above may apply to storm deposits (Kortekaas and Dawson, 2007; Morton et al., 2007). More significant differences appear when deposition and erosion are considered at the transect scale (dozens to hundreds of meters): storm deposits are commonly narrow thick deposits with abrupt landward thinning, whereas tsunami deposits are broader drapes displaying progressive landward thinning. The interpretation of coastal boulder accumulations also remains under discussions. The effects of storms, as described in Iceland (Etienne and Paris, 2010), Scotland and Ireland (Williams and Hall, 2004; Hall et al., 2006), appear well in excess of those generally reported in the literature. The tsunami origin is actually preferred, but few studies describe boulders deposition by recent tsunamis (Minoura et al., 1997; Goff et al., 2006b; Goto et al., 2007; Kelletat et al., 2007; Paris et al., 2009; Yawsangratt et al., 2009).

In this paper we present new data on sediment transport and deposition during the December 26, 2004 tsunami inflow and outflow in the Lhok Nga Bay (Fig. 1), located 10 km west of the city of Banda Aceh (northwest Sumatra, Indonesia). Side-scan sonar data of the near shore area are used to complete inland measurements, in particular for boulder transport.

2. Previous investigations in Lhok Nga

The Lhok Nga Bay is a 5 km large coastal embayment (25 km²) opened to the West and delimited by steep slopes. The coast prior to the 2004 tsunami appeared as a continuous beach, breached by small estuaries during the wet season. Main fringing reefs are located between Lampuuk and the Lhok Nga River. The lowest areas correspond to lagoons, swamps and rice crops. Small hills and hummocky terrains refer to dunes, beach ridges and palaeo-dunes reaching 15 m a.s.l. (e.g.

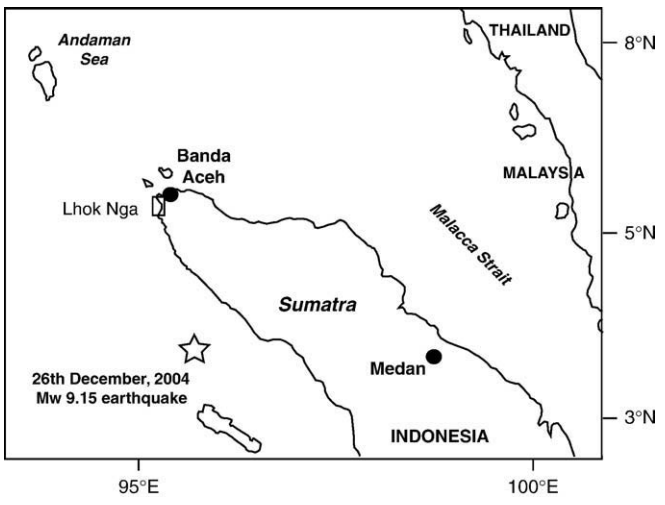

Fig. 1. Location map of the Lhok Nga Bay (northwest Sumatra, Indonesia).

Lampuuk, Lam Lho). In the southern part of the bay, the coastal morphology becomes more contrasted, especially south of the harbour, where the coast shows alternating cliffs and flat crescent-shaped bays and creeks.

The "Tsunarisk" franco-indonesian project conducted by Franck Lavigne and Raphaël Paris already published detailed reconstruction of the tsunami in Banda Aceh and Lhok Nga (Lavigne et al., 2009), descriptions and interpretation of coastal erosion, boulder and sand deposition in Lhok Nga and northeast Banda Aceh (Wassmer et al., 2007; Paris et al., 2007, 2009), SEM analysis of quartz grains (Costa et al., submitted for publication) and distribution of nannoliths in the tsunami deposits (Paris et al., 2010). Topographical and bathymetrical surveys were carried out in December 2005 and numerical modelling was carried out by the French "Commissariat à l'Energie Atomique" (Hébert et al., in press). In Lhok Nga, this model provides a grid of depth-averaged flow velocities each 5 min of simulation, with a spatial resolution of 18 m.

The December 26, 2004 tsunami in Sumatra was one of the largest tsunamis recorded in human history. In Lhok Nga, the tsunami waves were almost 30 m high and runups reached 51 m a.s.l. (Lavigne et al., 2009). Eyewitnesses reported 10 to 12 waves, the second and third ones being the highest. The sea was observed to recede 10 min after the earthquake and the first wave came from the southwest a few minutes later. The first wave moved rapidly landward as a turbulent flow 0.5 to 2.5 m deep. The second and largest wave (i.e. the tsunami bore) came from the west–southwest within 5 min after the first one and was 15–30 m high at the coast. Few eyewitness accounts are available for the outflow (backwash). Both inflow and outflow produced extensive erosion, sediment transport and deposition up to 5 km inland (Umitsu et al., 2007; Paris et al., 2009). The erosional imprints of the tsunami extend to 500 m from the shoreline and exceed 2 km along the river beds. The most eroded coasts were tangent to the tsunami wave train, which came from the southwest. The fringing reefs were not efficient in reducing erosion and destruction inland (Baird et al., 2005). The volume of beach eroded by the tsunami (ca. 1.5×10^5 m³ over 9.2 km of coast) represents less than 10% of the sediments deposited inland (ca. 1.5×10^6 m³).

The sandy deposits laid down by the tsunami inland record the successive inflows and a final outflow (the backwash), as shown by normally graded couplets or triplets of layers (Paris et al., 2007). The topmost layers, interpreted as the backwash deposition, describe a seaward sequence of increasing mean grain size and decreasing degree of sorting. Composition of the deposits and multi-modal grain-size distribution reflect different sources of sediments. The local effects of the topography on depositional conditions could be identified: thickest deposits in the topographic lows (50–80 cm), large-scale spatial variations in thickness and upper laminated texture when the sedimentation was limited by steep slopes, flame structures in the riverbeds, landward coarsening and very poor sorting at the wave breaking point.

The 2004 tsunami deposits in Lhok Nga are particularly rich in bioclasts: coral fragments, coral and sponge triaxones spicules, rhodophyta calcareous algae, nannoliths, diatoms, benthic foraminifers, gastropods, echinoderms and rare bryozoans. These faunistic and floristic species are typical of a shallow marine environment (Paris et al., 2007). Diatoms are often used to determine the marine provenance and sediment source of tsunami deposits (e.g. Dawson, 2007), but nannoliths can also help to interpret them (Paris et al., 2010). In Lhok Nga, the abundance of nannoliths in tsunami deposits tends to increase landward, from the shore to 1 km inland, and then decrease until the deposition limit. Nevertheless, the numbers of nannoliths, especially coccoliths, are highly variable when considered in vertical sections. On sections located near the coast, the arrival of the tsunami wave front is characterised by a decreasing number of coccoliths, rapidly followed by a peak of maximum abundance and a progressive decrease as water recedes. Further inland, the abundance of nannoliths decreases from base to top of the deposits, with pulses (successive waves) of higher abundance in finer sand layers.

The tsunami was also able to detach and transport coral boulders in excess of 10 t over 500–700 m and megaclasts from the tidal flat in excess of 85 t over a few meters (Paris et al., 2009). The coincidence of different size modes, from boulders to fine sands suggests that all the material was not transported in suspension, but rather through a combination of bed load and suspended transport modes. No landward fining trend in the boulder-size distribution could be detected. The spatial and size distributions of boulders mostly depend on the location and characteristics of their source (Fig. 2: coral reef, beach rock, platform, seawall), together with clast and surface interference during transport. The elongated boulders tend to be imbricated or have their long axis tangent to the direction of the flow.

3. Methodology

3.1. Morphometry and distribution of boulders offshore

Side-scan sonar and scuba-diving surveys were carried out in August 2006 (Fig. 3). An area of 8.6 km² off Lhok Nga was covered by a side-scan sonar Edge Tech type DF 1000 between 10 and 25 m deep (depending on weather conditions), with a 100 kHz frequency. The 20–25 cm resolution of images allows identifying boulders and other debris (including tree trunks and anthropogenic debris). We mapped and interpreted 7853 objects: 2894 anthropogenic debris, 1794 *in situ* blocks (small coral reefs and knolls, undetermined rocky platforms such as beach rock); 1760 boulders likely moved by the tsunami, 286 tree trunks and 1119 small debris not clearly determined. Despite a great variability in block shape and size, it is possible to distinguish *in situ* blocks and boulders moved by the tsunami. The main criteria are their shape, their position on the sea-bottom, their shadow, and their spatial distribution (see Section 4.2). *In situ* blocks from rocky platform are generally more or less egg-shaped, cast a well-defined linear shadow and seem to fit together. Boulders moved by the tsunami display sharp edges, and seem to be slightly buried in finer sediments. The criteria for transported vs. *in situ* blocks were tested during scuba-diving surveys on spots where both types were observed on the side-scan sonar imagery. However, we cannot completely rule out the hypothesis that some boulders were previously moved by recent storms or tsunamis.

We chose in a random way 302 boulders and measured for each boulder the visible longest and shortest axes (assimilated to A and B-axes, respectively). They were classified in 3 groups in order to test the relation location vs. size of the boulders (length and width): boulders deposited inland (data after Paris et al., 2009); submarine boulders from rocky outcrops (reefs and platforms) and transported offshore; *in situ* submarine blocks. In order to test the relation source vs. size of the boulders, we classified the boulders in 5 groups: boulders detached from coral reefs and knolls (G1: $n=45$); boulders detached from rocky platforms (G2: $n=45$); boulders delineating a large lobe south of the Lhok Nga Bay (G3: $n=43$); boulders deposited inland (G4: $n=80$); *in situ* blocks of rocky platforms (G5: $n=89$). Differences between means of morphometric parameters of each group were tested either using one-way ANOVA or non-parametric Kruskal–Wallis tests (KW). The assumptions of normality and homoscedasticity were verified with Kolmogorov–Smirnov/Lilliefors tests and Levene/Brown–Forsythe tests respectively. Post-hoc comparisons were performed through HSD Tukey test for N different (Spjotvoll/Stoline test) or non-parametric multiple comparison (SNK) tests according to the cases.

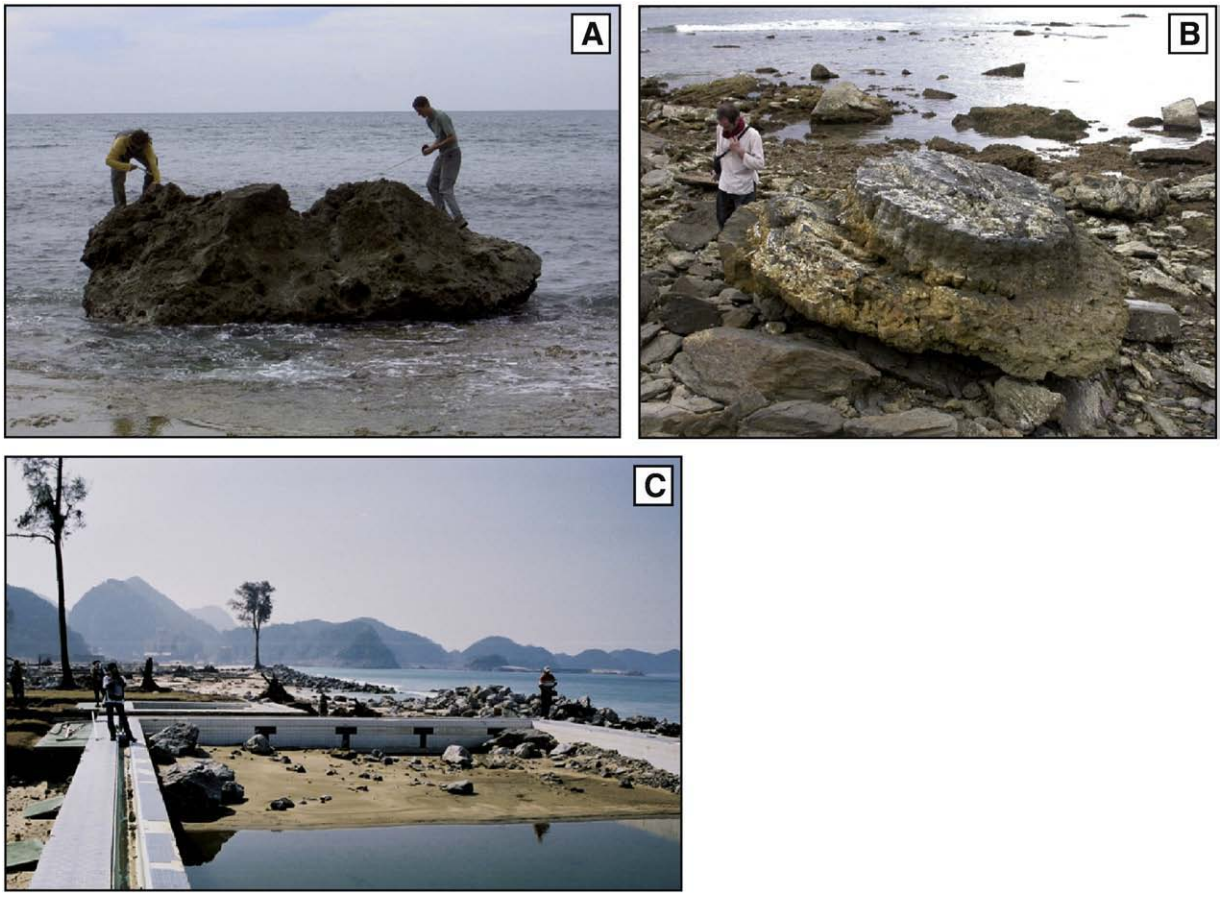

Fig. 2. Typology of boulders transported and deposited inland by the December 26, 2004 tsunami in Lhok Nga. A: Coral boulder found in overturned position; B: megaclasts from the tidal flat; C: calcareous boulders detached from a seawall (see shoreline in the background) and deposited in a swimming-pool at 4 m a.s.l.

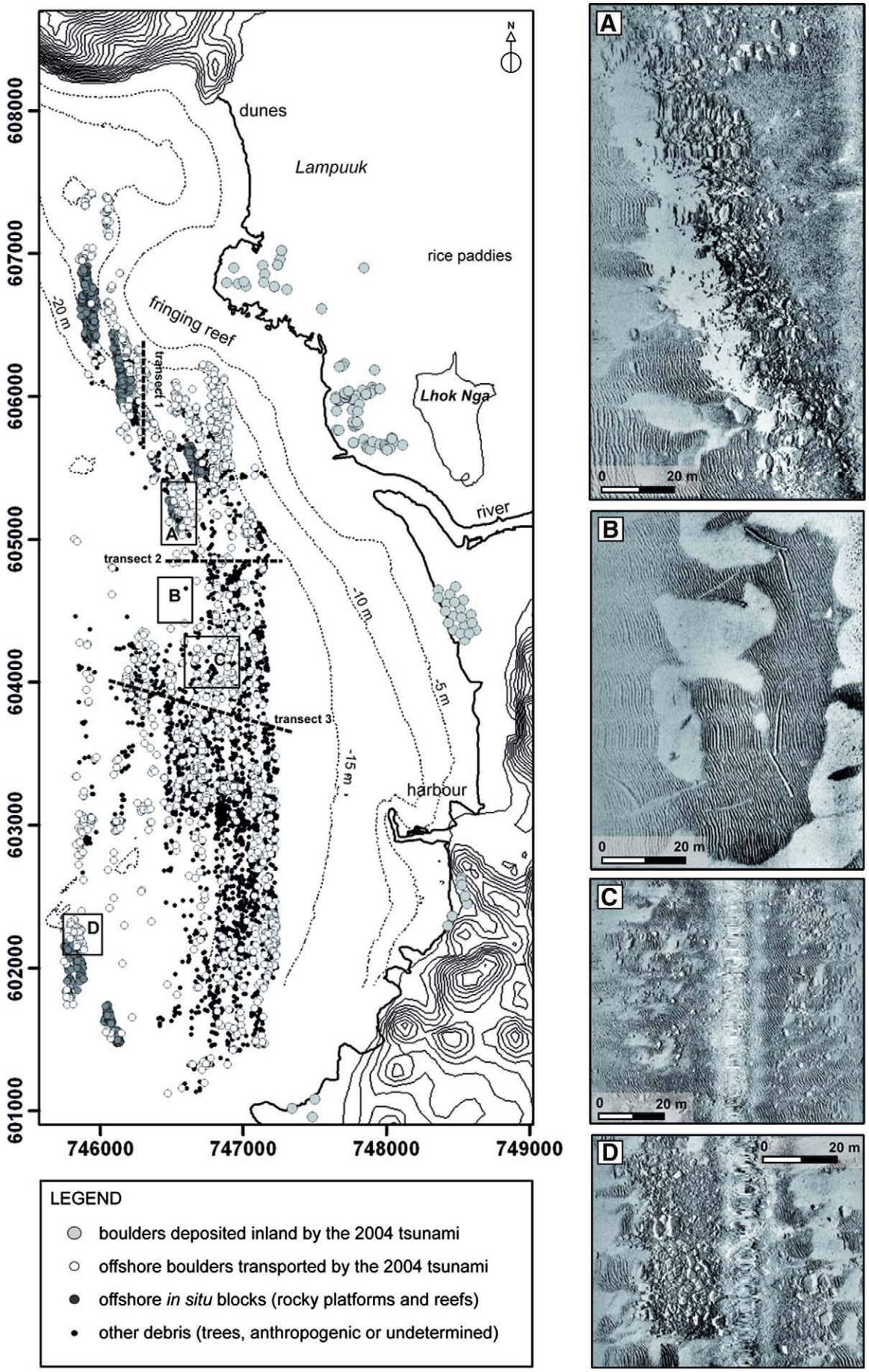
N
dunes
Lampuuk
rice paddies
fringing reef
-20 m
transect 1
Lhok Nga
river
A
transect 2
B
-10 m
-5 m
C
transect 3
-15 m
harbour
D
608000
607000
606000
605000
604000
603000
602000
601000
746000
747000
748000
749000
A
0
20 m
B
0
20 m
C
0
20 m
D
0
20 m
LEGEND
boulders deposited inland by the 2004 tsunami
offshore boulders transported by the 2004 tsunami
offshore *in situ* blocks (rocky platforms and reefs)
other debris (trees, anthropogenic or undetermined)

3.2. Modelling entrainment of fine sediments offshore

Tsunami waves create the bed shear velocities to levels above critical values for the entrainment of submarine sediments. We estimated the movable grain sizes based upon the simulated current velocities of the tsunami waves (e.g. Maeno and Imamura, 2007; Noda et al., 2007). We assumed that the flow type generated by the tsunami was a unidirectional flow, because the wave periods were very long, and that the predominantly sandy sediments behave in an essentially non-cohesive manner (sand ripples).

Threshold shear velocity (u_*) at the bed can be related to threshold flow velocity U_{100} (nominally taken as 100 cm above the bed) using Karman–Prandtle equation:

$$U_{100} = \frac{u_*}{\kappa}\ln\frac{z}{z_o}. \quad (1)$$

Critical threshold shear velocity (u_{*cr}) of each grain-size class (D) is then derived through the Shields (1936) entrainment function:

$$\theta_{cr} = \frac{\rho_w u_{*cr}^2}{(\rho_s-\rho_w)gD}. \quad (2)$$

Threshold Shields parameter θ_{cr} for cohesionless grains (e.g. Soulsby and Whitehouse, 1997) is given by:

$$\theta_{cr} = \frac{0.3}{1+1.2D_*} + 0.055\left(1-\exp[-0.020D_*]\right) \quad (3)$$

with dimension less grain size D_* (Yalin, 1972):

$$D_* = \left(\frac{(\rho_s-\rho_w)g}{\nu^2}\right)^{1/3} \quad (4)$$

where κ is von Karman's constant ($\kappa \approx 0.4$), z is the height above the bed (cm), z_o is the roughness length (cm), ρ_s is the density of the boulder (g/cm³: see Paris et al., 2009), ρ_w is the water density ($\rho_w = 1.025$ g/cm³ for sea water), g is the gravitational acceleration ($g = 9.8$ m/s²) and ν is the sea water viscosity at 25 °C (0.00896 m²/s). As observed by scuba diving and side-scan sonar, the study area offshore mostly displays rippled sands, except around the fringing reefs and rocky platforms. Thus, the model of threshold shear velocity was computed with a constant roughness length $z_o = 0.6$ (Yalin, 1972; Heathershaw, 1981). However, calculations of threshold shear velocity around fringing reefs and rocky platforms were also tested with different roughness lengths, but the effects are minor. We also assumed that the depth-averaged flow velocities given by the numerical simulation (Hébert et al., in press) are similar to threshold flow velocity U_{100}.

We thus illustrate the relationship between the critical threshold shear velocity (u_{*cr}) of a specific grain size (D) and the simulated tsunami shear velocity (u_*) each 5 min of simulation. Sediment transport occurs when $u_* > u_{*cr}$. We calculated and compared the critical threshold shear velocities of specific grain sizes and the simulated tsunami shear velocities using the 18 m bathymetric grid mentioned above.

3.3. Modelling megaclast transport

We applied the equations presented by Nott (2003) and Noormets et al. (2004) to the boulders deposited both inland and offshore by the 2004 tsunami. Forces acting on a boulder or megaclast impacted by a tsunami can be described as follows:

$$\text{Drag force}: F_D = C_d A_n(\rho_w u^2/2) \quad (5)$$

$$\text{Lift force}: F_L = C_1 A_p(\rho_w u^2/2) \quad (6)$$

$$\text{Inertia force}: F_I = \rho_w C_i V\dot{u} \quad (7)$$

$$\text{Resisting force}: F_R = (\rho_s-\rho_w)gV \quad (8)$$

$$\text{Frictional force}: F_\mu = \mu mg \quad (9)$$

where A_n is the area of the boulder projected normal to the flow (m²), A_p is the area of the boulder parallel to the flow (m²), u is the tsunami flow velocity at boulder initial location (m/s), $\dot{u}$ is the peak flow acceleration (1 m/s², following the results of Noji et al., 1985; Nott, 2003), V is the boulder volume (m³), C_d is the drag coefficient ($C_d = 1.95$ for submerged boulders), C_1 is the lift coefficient ($C_1 = 0.178$), C_i is the inertia coefficient ($C_i = 2$), μ is the friction coefficient ($\mu = 0.7$ after Noormets et al., 2004) and m is the boulder mass (kg).

The transport of megaclasts will be initiated when the balance of forces becomes unsteady. Three pre-transport environments of megaclasts can be distinguished that determine the flow velocity of wave required for them to be transported (Nott, 2003). Transport of submerged boulders will be initiated when:

$$F_D + F_L > F_R \quad (10)$$

and for subaerial boulders when:

$$F_D + F_L + F_I > F_R \quad (11)$$

and for joint-bounded blocks when:

$$F_L \geq F_R \quad (12)$$

Following Noormets et al. (2004), transport inland will theoretically stop when the fluid drag (F_D) is equal or less than the net friction (F_μ):

$$F_D \leq F_\mu. \quad (13)$$

Balancing Eqs. (5) and (9), the flow velocity required for moving boulders is defined by:

$$u = \sqrt{\left(\frac{2\mu mg}{C_d A_n \rho_w}\right)}. \quad (14)$$

We then used Nott's (2003) equations in order to estimate minimum wave height (H_t) required to initiate transport of:subaerial boulders:

$$H_t \geq \frac{0.25(\rho_s-\rho_w/\rho_w)2a}{C_d(ac/b^2)+C_l} \quad (15)$$

submerged boulders:

$$H_t \geq \frac{0.25(\rho_s-\rho_w/\rho_w)[2a-C_m(a/b)(u^\circ/g)]}{C_d(ac/b^2)+C_l} \quad (16)$$

Fig. 3. Boulders and other debris transported by the December 26, 2004 tsunami off Lhok Nga, mapped after side-scan sonar survey (August 2006). Isobaths 5 m after Lavigne et al. (2009). Snapshot A: *In situ* large blocks forming an elongated platform (old coral reef?); B: tree trunks perpendicular to post-tsunami sand ripples and buried by sand indicate the outflow direction and trunks parallel may have been removed by the northward longshore drift currents. C: Coral boulders transported by the 2004 tsunami (isolated or in clusters); D: boulders detached from a fractured rocky platform.

and joint-bounded blocks:

$$H_t \geq \frac{0.25(\rho_s - \rho_w / \rho_w)2a}{C_l} \quad (17)$$

where H_t is the height of tsunami wave at breaking point, a is the A-axis of the megaclasts, b the B-axis and c the C-axis (m), and C_m is the mass coefficient ($C_m = 2$ for subaerial boulders).

The 2004 tsunami in Lhok Nga transported three types of megaclasts (Paris et al., 2009). South of the main river mouth, subaerial calcareous boulders up to 7.7 tons (3.3 × 1.7 × 1.1 m, 3.2 m³) were lifted from a seawall and deposited until 200 m inland. The total amount of boulders transported may be over 1000, all located along a 250 m strip between the seawall and the main road. The lateral extension of the boulder field corresponds to the length of the seawall and the dispersion of boulders landward was limited. There is not a landward nor seaward fining of the boulders, but their distribution suggest little rearrangement by the tsunami outflow (Paris et al., 2009). South of Lhok Nga Harbour, tabular megaclasts up to 85 tons (7.2 × 5.2 × 2.1 m, 60 m³) were dislodged from the rocky platform and deposited to a few meters inland where they were found in overturned position (Paris et al., 2009). The submerged scars can be observed when the sea is calm. Thus, these megaclasts can be considered as pre-tsunami joint-bounded blocks. The submerged type is represented by coral boulders up to 11 tons (3.5 × 2.5 × 1.8 m, 10.5 m³) deposited as far as 900 m inland. Smaller coral boulders (<1 m) were found until 1460 m inland. Elongated boulders tend to dispose their long axis tangent to the direction of the tsunami inflow. Imbricate clusters also record inflow orientations, thus suggesting that few boulders left inland were transported by the backwash. We also applied the equations for submerged boulders to the largest boulders identified offshore. Boulder density was previously estimated onshore by Paris et al. (2009).

4. Results

4.1. Threshold shear velocities offshore

Tsunami waves created the bed shear velocities to levels above critical values of the entrainment of continental shelf sediments (Fig. 4). The arrival of the tsunami in the Lhok Nga Bay occurs 30 min after the earthquake in the numerical simulation (~20 min after eyewitness accounts: Lavigne et al., 2009). Threshold shear velocities of the tsunami bore offshore are already high enough ($u_* > 0.5$ cm/s) to mobilize all fractions of sand-size sediments ($u_{*cr} \approx 0.3$ cm/s for coarse sands). Then, very high values of u_* (10–20 cm/s) are observed at the coast, especially around the fringing reef in Lampuuk. The outflow (backwash) begins after 55 min of simulation and appears concentrated at the mouth of the main river and around the fringing reefs ($u_* > 20$ cm/s). A large lobe of lower values of u_* (<3 cm/s) appears in the south part of the bay, coinciding with the G3 boulder field (identified by side-scan sonar survey). The extent of the outflow reaches its maximum at 65–75 min. Very high values of u_* (>30 cm/s) suggest that large volume of sediments were reworked and re-deposited offshore during the outflow.

4.2. Size of offshore boulders according to their location and source

Do the length and width of boulders change with location? Results from one-way ANOVA show significant differences between the three groups for the A-axis ($F_{(2,299)} = 3.187$; $P < 0.05$; cube transformed data). Mean A-axis of submarine boulders transported (but not deposited inland) are significantly longer than A-axis of boulders measured on land (Paris et al., 2009). *In situ* submarine blocks and submarine transported boulders have larger B-axis than those on land (KW: $H_{(2,302)} = 124{,}486$; $P < 0.001$) (Table 1).

Do the length and width of boulders change with source? We found significant differences for the A-axis (KW: $H_{(4,302)} = 198{,}04$; $P < 0.001$) and B-axis (KW: $H_{(4,302)} = 188{,}93$; $P < 0.001$) between the five groups of boulders. Post-hoc comparison tests show that each group of boulders is significantly different from the others (Tables 2 and 3). Boulders eroded from coral reefs (G1) are larger than those from rocky platform (G2) but there are not significantly different than boulders G3 (lobe-shaped field south of the bay). Boulders from rocky platforms (G2) are smaller than isolate *in situ* blocks (G5). G3 are highly significantly larger than G4 boulders (deposited inland), but the G3 boulder field offshore is not associated to boulder accumulations onshore. This is concordant with the results of threshold shear velocities calculated during the outflow in this area.

4.3. Offshore boulder-size trends along transects

We measured the A- and B-axes of boulders ($n = 48$) along a 600 m long transect oriented South–North (perpendicular to the wave direction), from a rocky platform to the base of the Lampuuk fringing reef (Fig. 3: transect 1). Boulders were grouped according to their distance from rocky platform (a station every 100 m). Pearson's correlation analysis indicates that the A- and B-axes of boulders are not strongly correlated ($r = 0.46$; $P < 0.001$). A significant negative correlation was found between the two axes and the distance to the rocky platform ($r = -0.43$; $P < 0.005$ for A-axis and $r = -0.28$; $P < 0.05$ for B-axis). The differences of means of A- and B-axes between each station were not significant (one-way ANOVA). No clear boulder-size gradient was found from the rocky platform to the fringing reef, despite the results of correlations.

We made another transect oriented West–East from a rocky platform toward the coast (Fig. 3: transect 2) and measured the A- and B-axes of the boulders ($n = 36$). A Pearson's correlation analysis show a correlation between the two axes ($r = 0.62$; $P < 0.00005$). No significant correlation was found between the axes of boulders and distance. A one-way ANOVA does not show any difference in the mean axes between boulder groups with distance from the rocky platform. No boulder-size gradient was found for this transect.

In order to infer the boulder-size distribution of the G3 boulder field, we measured the A-axis and B-axis of boulders ($n = 81$) along a 1200 m long transect oriented WNW–ESE (Fig. 3: transect 3). The Pearson's correlation analysis shows that A- and B-axes of boulders are strongly correlated ($r = 0.87$; $P < 0.00001$). A significant positive correlation was also found between the two axes and the distance to the coastline ($r = 0.61$; $P < 0.000000001$ for A-axis and $r = 0.63$; $P < 0.00001$ for B-axis). Boulders up to 5.5 m, 7 m and 14.8 m large (A-axis) were identified at 2400 m, 2300 m and 1950 m respectively from the coast. A Multiple linear regression (MLR) confirms this highly significant relationship ($R^2 = 0.42$; $F_{(2,78)} = 28{,}10$; $P < 0.000001$) between the boulder size and the distance to the coastline (Fig. 5). The largest boulders are located at the front of the accumulation (seaward edge), where the density of boulders is particularly high (Figs. 3 and 6). This coarse frontal zone appears between 2200 and 2400 m from the coast (Fig. 5). The equations of regression are $Y = -1.3237 + 0.0011\,X$

Fig. 4. Maps of threshold shear velocity values (u_*) for a roughness length $z_o = 0.6$ cm. Low values appear in blue and high values in red. 30 min after the main earthquake, the tsunami wave train approaches Lhok Nga. u_* are already high enough (>0.5 cm/s) to mobilize submarine sediments (u_{*cr} of very coarse sands is ≈0.3 cm/s). At 40–45 min, the tsunami has invaded the Lhok Nga Bay and high values of u_* (10–20 cm/s) are observed at the coast, especially around the fringing reef in Lampuuk. At 55 min, the outflow (backwash) begins (river mouth and fringing reefs). A large lobe of low values of u_* (<3 cm/s) appears in the south part of the bay, coinciding with the G3 boulder field (identified by side-scan sonar survey). After more than 65 min of simulation, the extent of the outflow reaches its maximum and very high values of u_* (>30 cm/s) suggest that large volume of sediments were reworked and re-deposited offshore. (For interpretation of the references to colour in this figure legend, the reader is referred to the web version of this article.)

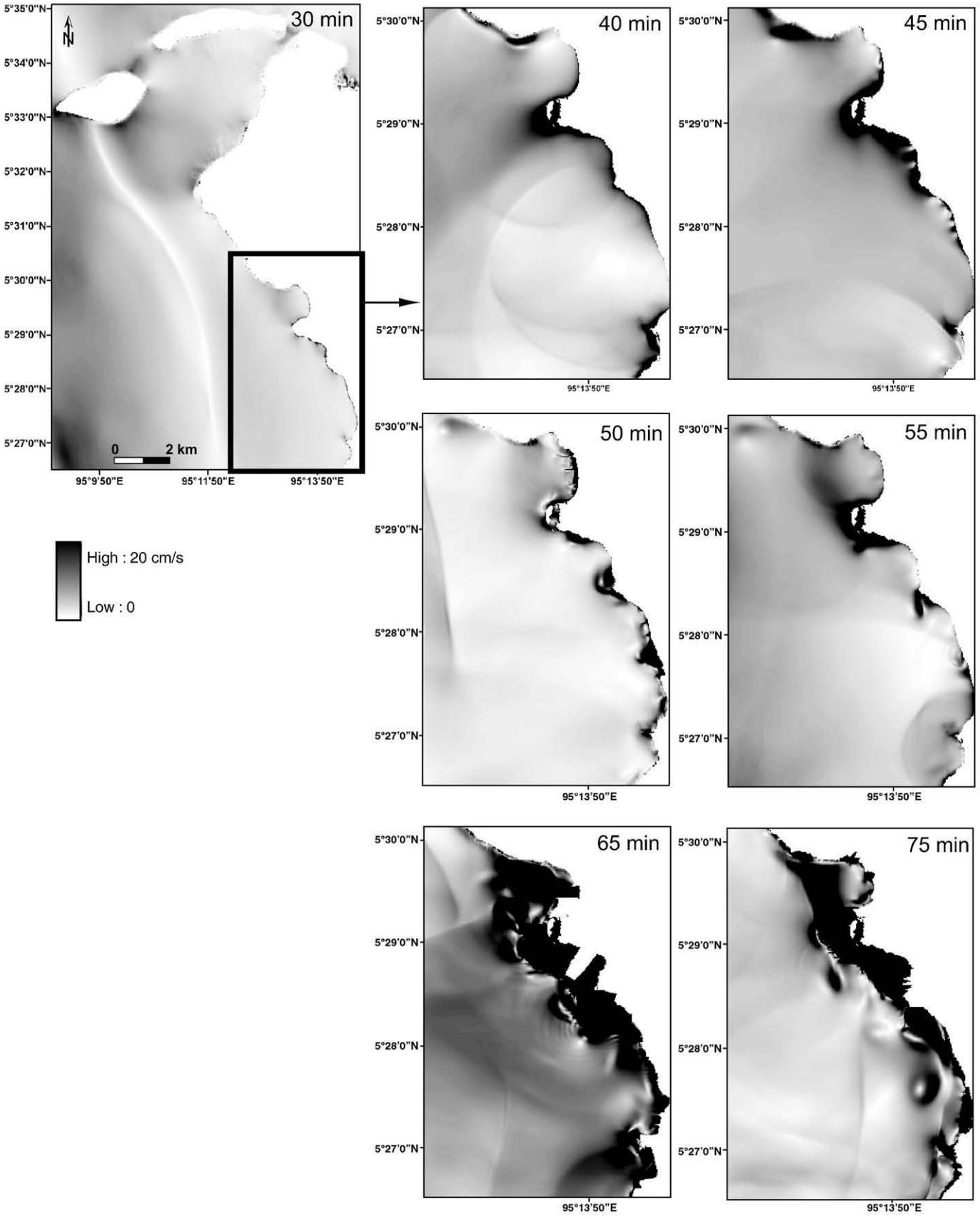
30 min
40 min
45 min
50 min
55 min
65 min
75 min
N
0 2 km
High : 20 cm/s
Low : 0
5°35'0"N
5°34'0"N
5°33'0"N
5°32'0"N
5°31'0"N
5°30'0"N
5°29'0"N
5°28'0"N
5°27'0"N
95°9'50"E
95°11'50"E
95°13'50"E

Table 1
Mean morphometric parameters (±SD) of the boulders expressed for each position on the coast and results of multiple comparison tests (HSD Tukey or SNK post-hoc comparison) (S: whole test significant; *: multiple comparison tests significantly different).

Morphometric parameters of boulders	Submarine boulders transported (1)	*In situ* submarine blocks (2)	Boulders deposited inland (3)	Means comparisons			
A-axis	4.26 (2.92)	4.16 (1.61)	1.06 (0.67)	ANOVA	S	*1 3	$P<0.05$
B-axis	2.29 (1.33)	2.30 (0.71)	0.81 (0.52)	KW	S	*1 3	$P<0.000001$
						*2 3	$P<0.01$

for the A-axis (log transformed data) ($P<0.05$) and $Y=-1.3855+0.0009\,X$ for the B-axis (log transformed data) ($P<0.05$). We also compared the differences of means of A- and B-axes of boulders between each station along the western–eastern transect. One-way ANOVA reveals highly significant differences for A-axis ($F_{(9,71)}=10.04$; $P<0.000001$; log transformed data) and B-axis ($F_{(9,71)}=13.25$; $P<0.000001$; log transformed data). The boulders located at the edges and front of the debris lobe are significantly larger ($P<0.05$) and longer ($P<0.005$) than those of the central part of the accumulation field, where the density of boulders is also lower.

4.4. Tsunami flow velocities and wave heights

Tsunami flow velocities required for initiating the transport of the largest boulders observed both on land and offshore are in good agreement with the flow velocities at boulder source (Table 4), estimated using numerical modelling and eyewitness accounts (Hébert et al., in press; Paris et al., 2009). After Eq. (14), velocities higher than ~4 m/s are required to move the coral boulders from the Lampuuk fringing reefs (north part of the bay) and the calcareous boulders from the seawall (central part of the bay). Numerical models give tsunami flow velocities increasing from 3 to 12 m/s from the coral boulder fields offshore to the coast. Thus, larger clast than those observed (if available) could have been moved by the tsunami inflow. Megaclasts detached from the tidal flat south of the harbour have been transported over a few meters, and this is in good agreement with the very small difference observed between the numerical model (3–7 m/s) and the mechanical model given by Eq. (14) (>6.2 m/s). The same method applied to the largest boulders identified offshore also gives reasonable results: the transport of the largest boulders can start if flow velocities are higher than 7.5 m/s. Both inflow and outflow produced such velocities, except for the area where the G3 lobe was formed (<6 m/s).

Using the dimensions and mass of the largest boulders observed (Eq. (14)), transport should stop when the flow velocity $u\leq 3$ m/s for coral boulders deposited inland, $u\leq 4$ m/s for calcareous boulders from the seawall, $u\leq 5$ m/s for joint-bounded megaclasts from the tidal flat, and $u\leq 7$ m/s for boulders deposited offshore. The model seems applicable to the boulders of the G3 lobe, for which the deposition during tsunami outflow ends at 75% of the theoretical transport distance ($u=7$ m/s at 3200 m from the coast). In other settings, the distances covered by the boulders inland are not in agreement with the high flow velocities, both during phases of inflow (e.g. 8–15 m/s in Lampuuk where no boulders were found more than 1500 m inland) or outflow (e.g. 8–21 m/s at the exit of the fringing reefs). The transport distance appears to be controlled by clast-to-clast interactions and by the topography (reefs, slopes, roads, large *Casuarina* trees, etc. may stop transport prematurely).

The minimum wave heights given by Nott's equations (2003) are considerably lower (>0.3 m for coral boulders found inland, >0.8 m for calcareous boulders from the seawall, >4.0 m for joint-bounded megaclasts from the tidal flat, >4 m for the coral boulders offshore) than the heights measured at the coast (>15–30 m) or simulated offshore (>8 m at 2 km from the coast). Thus, wave heights calculated by Nott's method appear underestimated and should be applied with caution, especially for hazard assessment and interpretation of coastal boulder accumulations.

Table 2
Mean morphometric parameters (±SD) of the boulders expressed for each defined group of boulders.

Morphometric parameters of blocks	G1	G2	G3	G4	G5
	Boulders from coral reefs	Boulders from rocky platforms	Other transported boulders	Boulders deposited inland	*In situ* blocks of rocky platforms
A-axis	4.23 (1.97)	2.37 (0.95)	6.27 (3.73)	1.06 (0.67)	4.16 (1.61)
B-axis	2.24 (0.76)	1.23 (0.56)	3.47 (1.41)	0.81 (0.52)	2.30 (0.71)

5. Discussion

5.1. Sediment sources and budget

The 2004 tsunami carried a large amount of sediments and debris. Eyewitness accounts recall waves already black before breaking inland (Lavigne et al., 2009). The simulation of threshold shear velocities suggests that most of the sediments deposited inland may have come from offshore, from fine sands to coral boulders. In a previous contribution (Paris et al., 2009), we estimated that the volume of beach eroded by the tsunami (ca. 0.15×10^6 m³) represented less than 10% of the sediments deposited inland (ca. 1.5×10^6 m³). Nevertheless, the coastal and shallow-water signature of the nannolith communities (Paris et al., 2010) indicates that there is not an increase of open-ocean over coastal taxa brought by the tsunami. Thus, there is no major transport of silty–clay size equivalent particles from furthest offshore during the tsunami event (i.e. off the continental shelf, the isobath −60 m being located at 22 km from the coast). Despite high shear velocities of the tsunami, the continental slope may have limited sediment transport upward from the Aceh basin (2700–2300 m deep) to the fore arc shelf (depth <200 m).

According to threshold shear velocities, the outflow may have reworked and re-deposited significant volumes of sediments offshore (probably more than the volume laid down on land in areas severely affected by the outflow). Flame structures oriented seaward observed in tsunami deposits of the Lampuuk river suggest an unidirectional outflow with sufficiently high shear velocities to deform unconsolidated substrate in riverbeds (see figure 11 in Paris et al., 2007).

The side-scan sonar survey coupled with investigations of boulder deposits on land reveal that all rocky outcrops offshore were affected by the tsunami (up to 25 m deep). The amount of boulders transported from offshore and deposited on land represents only 7% of the total number of boulders moved during the tsunami. Feldens et al. (2009) suggested that some boulders found in channels off Cape Pakarang (Thailand) were transported by the 2004 tsunami outflow. However, we could not find clear evidences of boulder motion during the outflow, except for the southern part of the bay (G3 lobe). The

Table 3
Results of multiple comparison tests (SNK post-hoc comparison) between each defined group of boulders from KW tests, with *P* value (N.S.: non significant).

Means comparisons								
	A-axis				B-axis			
	G1	G2	G3	G4	G1	G2	G3	G4
G2	$P<0.0005$				$P<0.00005$			
G3	N.S.	$P<0.00001$			$P<0.05$	$P<0.00001$		
G4	$P<0.000001$	$P<0.0005$	$P<0.000001$		$P<0.00001$	N.S.	$P<0.000001$	
G5	N.S.	$P<0.0001$	N.S.	$P<0.00001$	N.S.	$P<0.0001$	$P<0.01$	$P<0.00001$

elongated boulders deposited inland tend to dispose their long axis tangent to the tsunami inflow (Paris et al., 2009), and the distribution of boulder accumulations is connected to the boulder sources available during the tsunami inflow (fringing reefs, platforms, isolated knolls etc.).

5.2. Subaqueous sedimentary density flows and tsunamis

Because of its characteristics (lobe-shaped accumulation, higher density and larger boulders at the front and edges, seaward coarsening), we interpret the G3 boulder field as the deposit of subaqueous sedimentary density flow (Mulder and Alexander, 2001) formed during the tsunami outflow. The thickness of the boulder accumulation cannot be estimated, but it covers an area of 3.5 km². The occurrence of a density flow in the southern part of the bay can be explained by interactions between the tsunami wave and the topography. Where inflow deposition was limited by steep slopes near the coast (e.g. near the harbour), the outflow was saturated in debris. Side-scan sonar images reveal high concentrations of debris (anthropogenic debris, tree trunks, and boulders) between the Lhok Nga river mouth and the harbour. A multi-lobe mass of debris propagating seaward appears on the Spot-2 scene took 3 h after the tsunami (Fig. 6). The G3 boulder field may correspond to the final deposition of these lobes up to 2400 m from the coastline, where sea-bottom slope becomes lower than 2°, at 22 m deep. The very dense sediment–water mixture may have behaved as a Bingham fluid dominated by shearing and frictional debris interactions. These cohesive lobes observed on Spot-2 scene may have then transformed into non-cohesive and less-concentrated flows without boulders. The distribution of other boulder accumulations is more likely guided by submarine morphology, such as fringing reefs and rocky platforms (Fig. 6).

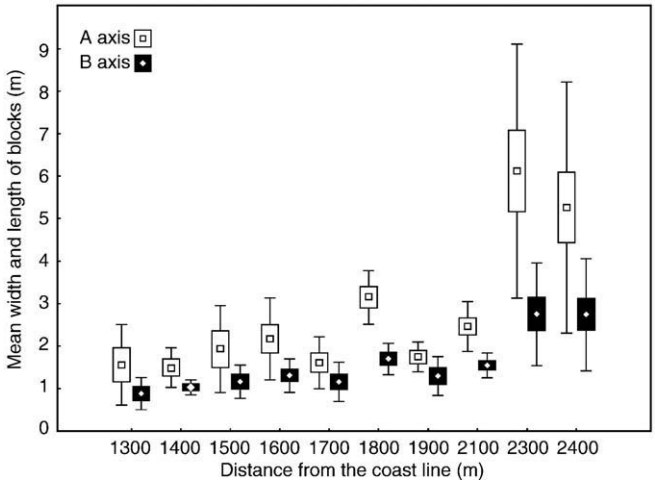

Fig. 5. Box-plot of boulder size along East–West transect 3 in the G3 boulder field (mean, box: mean ± Er-type, mean ± Std-error). Error-type (Er-type) is an estimation of the standard deviation between measured values and true values. The Standard-error (Std-error) is a measure of the magnitude of the error of an estimated statistic.

This may be the first observation of a subaqueous sedimentary density flow formed during the outflow of a recent tsunami. Deposits interpreted as density flows during tsunamis are already described in the literature. Debris-flow conglomerates with shear carpet indicating very dense and highly sheared fluid with possible Bingham characteristics were described in Chile (Le Roux et al., 2004; Le Roux and Vargas, 2005). Shiki and Yamazaki (1996) described in detail tsunami-induced conglomerates in central Japan. Debris-flow deposits, 40–80 cm thick, with clasts up to 50 cm and cobble fabrics seaward, were also interpreted as the result of a tsunami outflow on the western coast of Gran Canaria (Paris et al., 2004). Tanner and Calvari (2004) also interpret coarse breccias on the steep slopes of Stromboli Island as generated by the outflow of a tsunami. Cantalamessa and Di Celma (2005) described a boulder-bearing breccia laid down by subaqueous density flow during tsunami outflow in northern Chile. Feldens et al. (2009) observed stiff mud deposits with grass, woods and shells transported by density flows in channels parallel to the 2004 tsunami outflow in Thailand (Pakarang Cape).

5.3. Keys for identifying and interpreting palaeo-tsunamis

The emplacement of coastal boulder accumulation is usually attributed to high-energy events (tsunamis, hurricanes or powerful storms). However, their interpretation remains difficult along coasts where both storms and tsunamis occurred in the Past; especially when high-stand marine deposits are also present (Felton, 2002). A fundamental distinction between storms and tsunamis could be their capability of forming ridges (Etienne and Paris, 2010). Indeed, the organization of coarse clasts into ridges requires repeated reworking by waves rather than the single impact of a tsunami front wave (Williams and Hall, 2004). As far as we know, recent tsunamis did not leave boulder ridges. Goto et al. (2007) and Yawsangratt et al. (2009) described boulders lined up in rows after the 2004 tsunami in Thailand, but these boulders were not organised in ridges. Along the western coast of Sumatra, cobble-to-pebble ridges where deposited by storms on rocky coasts and behind fringing reefs during weeks and months that followed the 2004 tsunami (Paris et al., 2010). The extensive cobble-to-boulder ridges and ramparts described by Scheffers (2004) in the Leeward Netherlands Antilles are the only ridge-like features attributed to tsunamis so far studied. Nevertheless, Spiske et al. (2008) accurately calculated the density and porosity of these boulders and found that a hurricane origin was more likely than a tsunami origin.

Our results confirm that characteristics of boulders moved by a tsunami can help to estimate flow velocities required for detaching them. However, calculations of flow depth and transport distance do not provide convincing results. When considering their size and weight, boulders deposited by the 2004 tsunami in Lhok Nga may have been attributed to powerful storms. Nevertheless, their spatial distribution excludes the storm origin. More than 80% of the boulders are located more than 100 m inland. Furthermore, only large tsunamis

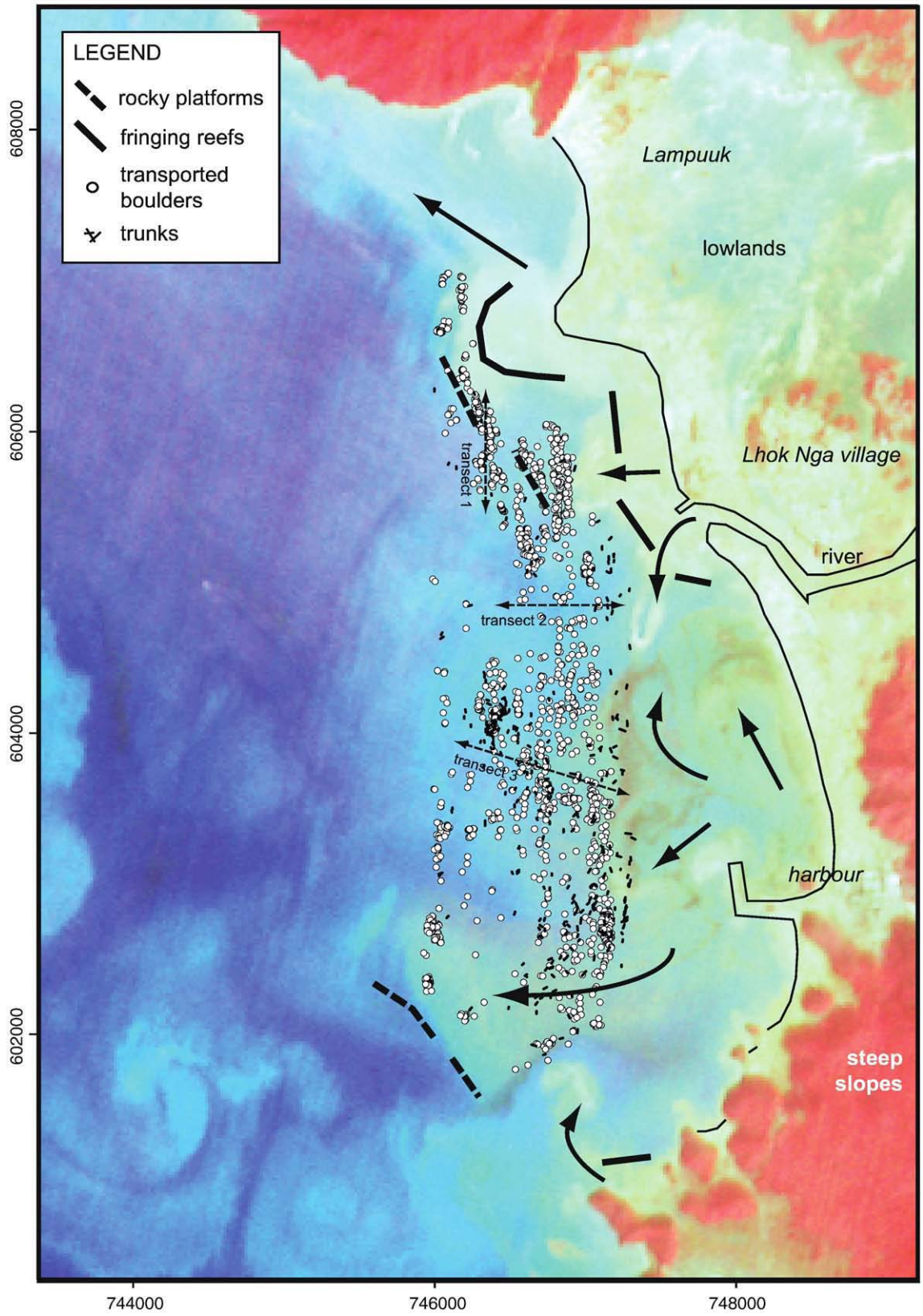

Fig. 6. Spot-2 scene took 3 h after the 2004 tsunami in the southern part of the Lhok Nga Bay. Note subaqueous sedimentary density flows, from cohesive density flows to turbidity currents, near the fringing reefs, at the mouth of the Lhok Nga River and north of the harbour. The G3 boulder field (transect 3) appears at the prolongation of multi-lobe density flows associated with the tsunami outflow. Inflow deposition was limited by steep slopes near the coast, and the outflow was thus saturated in debris. Main accumulations of tree trunks are associated with density flows from the Lhok Nga river, southwest of the harbour, and at the front of the G3 boulder field.

Table 4
Tsunami flow velocities estimated after the characteristics of the largest boulders transported and deposited both offshore and inland, compared with flow velocities estimated after numerical modelling and eyewitness accounts.

Boulder setting	Tsunami flow velocity (m/s)	
	From numerical modelling and eyewitness accounts	From characteristics of boulders (Eq. (14))
Coral boulders deposited inland	3–12	>3.7
Calcareous boulders from seawall	3–8	>3.9
Joint-bounded megaclasts from tidal flat	3–7	>6.2
Coral boulders identified offshore	8–13	>7.5

have sufficient flow velocities to transport numerous boulders offshore (at 15–25 m deep). We suggest that future studies coupling offshore–onshore mapping of boulder accumulations with reconstitutions of the morphological history (sea-level variations, coastal sediment discharge and landform evolution) may allow distinguishing palaeo-storm and palaeo-tsunami deposits.

A key issue in distinguishing large tsunamis from other processes could be their geomorphic and sedimentologic impact, both offshore and on land. Little is known about the response and resilience of coastal environments to high-energy events such as tsunamis. The initial geomorphic impact depend on the magnitude and duration of the event, but also on the physical vulnerability of coastal landforms (e.g. amplification of long waves by submarine canyons or bays, geometry of coral reefs, tidal flats acting as launching ramps for boulder accumulations, mangroves and forests reducing flow velocity etc.). Long-term geomorphic imprint may depend on thresholds, coastal environments being tsunami-resilient or storm-resilient under certain conditions of recurrence and magnitude. The recognition and study of past geomorphic crisis could then help in identify palaeo-tsunamis and assess their magnitude. Despite the exceptional magnitude of the 2004 tsunami, surveys carried out twenty months after the 2004 tsunami suggest that the coastal environment of Sumatra is tsunami-resilient, except for areas severely affected by land subsidence (due to the earthquake). The shoreline and coastal accumulations are now controlled by the climate seasonality and have a similar geometry as prior to the tsunami (Wassmer et al., 2007). Similar rapid beach recovery following the 2004 tsunami was observed in Thailand (Kotwicki and Szczuciñski, 2006). Even though large amounts of sediments were mobilized by the tsunami, only a minor volume was left on land. Sediments removed seaward by the outflow provided material for the beaches to recover rapidly. Side-scan sonar imagery of August 2006 at Lhok Nga displays sand ripples controlled by the longshore drift currents and the only surface evidences of the 2004 tsunami are the boulder accumulations. Finer deposits may have been preserved in sediment traps offshore and/or covered by post-tsunami sediments, and their recognition elsewhere would represent a way to identify great-magnitude tsunamis.

Acknowledgements

Funding came from the *Délégation Interministérielle pour l'Aide Post-Tsunami* (DIPT, project no. 161), the French Embassy in Indonesia and the *Centre National de la Recherche Scientifique* (CNRS) in France, in the framework of Tsunarisk and ATIP projects coordinated by Franck Lavigne and Raphaël Paris. We thank Fukashi Maeno for helpful discussions on sediment transport modelling. Comments by Witold Szczucinski and an anonymous reviewer significantly improved the earlier version of this paper. Finally, we would like to dedicate this contribution to our colleague and friend Rino Cahyadi.

References

Bahlburg, H., Weiss, R., 2006. Sedimentology of the December 26, 2004 Sumatra tsunami deposits in eastern India (Tamil Nadu) and Kenya. International Journal of Earth Sciences 96 (6), 1195–1209.
Baird, A.H., Campbell, S.J., Anggoro, A.W., Ardiwijaya, R.L., Fadli, N., Herdiana, Y., Kartawijaya, T., Mahyiddin, D., Mukminin, A., Pardede, S.T., Pratchett, M.S., Rudi, E., Siregar, A.M., 2005. Acehnese reefs in the wake of the Asian tsunami. Current Biology 15, 1926–1930.
Cantalamessa, G., Di Celma, C., 2005. Sedimentary features of tsunami backwash deposits in a shallow marine Miocene setting, Mejillones Peninsula, northern Chile. Sedimentary Geology 178, 259–273.
Choowong, M., Murakoshi, N., Hisada, K., Charoentitirat, T., Charusiri, P., Phantuwongraj, S., Wongkok, P., Choowong, A., Subsayjun, R., Chutakositkanon, V., Jankaew, K., Kanjanapayont, P., 2008a. Flow conditions of the 2004 Indian Ocean tsunami in Thailand, inferred from capping bedforms and sedimentary structures. Terra Nova 20, 141–149.
Choowong, M., Murakoshi, N., Hisada, K., Charusiri, P., Charoentitirat, T., Chutakositkanon, V., Jankaew, K., Kanjanapayont, P., Phantuwongraj, S., 2008b. 2004 Indian Ocean tsunami inflow and outflow at Phuket, Thailand. Marine Geology 248, 179–192.
Costa, P.J.M., Paris, R., Andrade, C., Freitas, M.C., Mahaney, W., Dawson, A., Voldoire, V., submitted for publication. SEM discrimination of coastal deposits: defining the high energy tsunami grain. Sedimentology.
Dawson, S., 2007. Diatom biostratigraphy of tsunami deposits: examples from the 1998 Papua New Guinea tsunami. Sedimentary Geology 200, 328–335.
Etienne, S., Paris, R., 2010. Boulder accumulations related to storms on the south coast of the Reykjanes Peninsula (Iceland). Geomorphology 114, 55–70.
Feldens, P., Schwarzer, K., Szczucinski, W., Stattegger, K., Sakuna, D., Somgpongchaiykul, P., 2009. Impact of the 2004 Indian Ocean tsunami on seafloor morphology and sediments offshore Pakarang Cape, Thailand. Polish Journal of Environmental Studies 18 (1), 63–68.
Felton, E.A., 2002. Sedimentology of rocky shorelines: 1. A review of the problem, with analytical methods, and insights gained from the Hulopoe Gravel and the modern rocky shoreline of Lanai, Hawaii. Sedimentary Geology 152, 221–245.
Goff, J., Liu, P., Higman, B., Morton, R., Jaffe, B., Fernando, H., Lynett, P., Fritz, H., Synolakis, C., Fernando, S., 2006a. Sri Lanka field survey after the December 2004 Indian Ocean tsunami. Earthquake Spectra 22, S155.
Goff, J.R., Dudley, W.C., deMaintenon, M.J., Cain, G., Coney, J.P., 2006b. The largest local tsunami in 20th century Hawaii. Marine Geology 226, 65–79.
Goto, K., Chavanich, S.A., Imamura, F., Kunthasap, P., Matsui, T., Minoura, K., Sugawara, D., Yanagisawa, H., 2007. Distribution, origin and transport process of boulders deposited by the 2004 Indian Ocean tsunami at Pakarang Cape, Thailand. Sedimentary Geology 202, 821–837.
Hall, A.M., Hansom, J.D., Williams, D.M., Jarvis, J., 2006. Distribution, geomorphology and lithofacies of cliff-top storm deposits: examples from the high-energy coasts of Scotland and Ireland. Marine Geology 232, 131–155.
Heathershaw, A.D., 1981. Comparisons of measured and predicted sediment transport rates in tidal currents. Marine Geology 42, 75–104.
Hébert, H., Brunstein, D., Loevenbruck, A., Sladen, A., Roger, J., Schindelé, F., Lavigne, F., Vautier, F., in press. Modélisation numérique du tsunami du 26 Décembre 2004 dans les districts de Banda Aceh et Lhok Nga (Sumatra, Indonésie). In: Lavigne, F., Paris, R. (eds), Tsunarisque: le tsunami du 26 décembre 2004 à Aceh, Indonésie. Publications de la Sorbonne, Paris.
Hori, K., Kuzumoto, R., Hirouchi, D., Umitsu, M., Janjirawuttikul, N., Patanakanog, B., 2007. Horizontal and vertical variations of 2004 Indian tsunami deposits: an example of two transects along the western coast of Thailand. Marine Geology 239, 163–172.
Huntington, K., Bourgeois, J., Gelfenbaum, G., Lynett, P., Yeh, H., Jaffe, B., Weiss, R., 2007. Sandy signs of a tsunami's onshore depth and speed. Eos, Transactions, American Geophysical Union 88 (52), 577–578.
Jaffe, B.E., Gelfenbaum, G., 2007. A simple model for calculating tsunami flow speed from tsunami deposits. Sedimentary Geology 200, 347–361.
Kelletat, D., Scheffers, S.R., Scheffers, A., 2007. Field signatures of the SE-Asian megatsunami along the West Coast of Thailand compared to Holocene paleo-tsunami from the Atlantic region. Pure and Applied Geophysics 164, 413–431.
Kortekaas, S., Dawson, A.G., 2007. Distinguishing between tsunami and storm deposits: an example from Martinhal, SW Portugal. Sedimentary Geology 200 (3–4), 208–221.
Kotwicki, L., Szczuciñski, W., 2006. Meiofaunal assemblages and sediment characteristics of sandy beaches on the West coast of Thailand after the 2004 tsunami event. Phuket Marine Biology Centre of Research Bulletin 67, 39–47.
Lavigne, F., Paris, R., Grancher, D., Wassmer, P., Brunstein, D., Vautier, F., Leone, F., Flohic, F., De Coster, B., Gunawan, T., Gomez, Ch., Setiawan, A., Cahyadi, R., Fachrizal, 2009. Reconstruction of tsunami inland propagation on December 26, 2004 in Banda Aceh, Indonesia, through field investigations. Pure and Applied Geophysics 166, 259–281.
Le Roux, J.P., Vargas, G., 2005. Hydraulic behavior of tsunami backflows: insight from their modern and ancient deposits. Environmental Geology 49, 65–75.
Le Roux, J.P., Gómez, C., Fenner, J., Middleton, H., 2004. Sedimentological processes in a scarp-controlled rocky shoreline to upper continental slope environment, as revealed by unusual sedimentary features in the Neogene Coquimbo Formation, north-central Chile. Sedimentary Geology 165, 67–92.
Maeno, F., Imamura, F., 2007. Numerical investigations of tsunamis generated by pyroclastic flows from the Kikai caldera, Japan. Geophysical Research Letters 34, L23303. doi:10.1029/2007GL031222.

Minoura, K., Imamura, F., Takahashi, T., Shuto, N., 1997. Sequence of sedimentation processes caused by the 1992 Flores tsunami: evidence from Babi Island. Geology 25 (6), 523–526.
Moore, A., Nishimura, Y., Gelfenbaum, G., Kamataki, T., Triyono, R., 2006. Sedimentary deposits of the 26 December 2004 tsunami on the northwest coast of Aceh, Indonesia. Earth Planets and Space 58, 253–258.
Morton, R.A., Gelfenbaum, G., Jaffe, B.E., 2007. Physical criteria for distinguishing sandy tsunami and storm deposits using modern examples. Sedimentary Geology 200, 184–207.
Morton, R.A., Goff, J.R., Nichol, S.L., 2008. Hydrodynamic implications of textural trends in sand deposits of the 2004 tsunami in Sri Lanka. Sedimentary Geology 207 (1–4), 56–64.
Mulder, T., Alexander, J., 2001. The physical character of subaqueous sedimentary density flows and their deposits. Sedimentology 48, 269–299.
Nanayama, F., Shigeno, K., 2006. Inflow and outflow facies from the 1993 tsunami in southwest Hokkaido. Sedimentary Geology 187, 139–158.
Noda, A., Katayama, H., Sagayama, T., Suga, K., Uchida, Y., Satake, K., Abe, K., Okamura, Y., 2007. Evaluation of tsunami impacts on shallow marine sediments: an example from the tsunami caused by the 2003 Tokachi-oki earthquake, Northern Japan. Sedimentary Geology 200, 314–327.
Noji, M., Imamura, N., Shuto, N., 1985. Numerical simulation of movement of large rocks transported by tsunamis. Proceedings of the IUGG/IOC International Tsunami Symposium, Wakayama, Japan, pp. 189–197.
Noormets, R., Crook, K.A.W., Felton, E.A., 2004. Sedimentology of rocky shorelines: 3. Hydrodynamics of megaclasts emplacement and transport on a shore platform, Oahu, Hawaii. Sedimentary Geology 172, 41–65.
Nott, J., 2003. Waves, coastal boulders and the importance of the pre-transport setting. Earth and Planetary Science Letters 210, 269–276.
Paris, R., Pérez Torrado, F.J., Cabrera, M.C., Schneider, J.L., Wassmer, P., Carracedo, J.C., 2004. Tsunami-induced conglomerates and debris flow deposits on the western coast of Gran Canaria (Canary Islands). Acta Vulcanologica 16 (1), 133–136.
Paris, R., Lavigne, F., Wassmer, P., Sartohadi, J., 2007. Coastal sedimentation associated with the December 26, 2004 in Lhok Nga, west Banda Aceh (Sumatra, Indonesia). Marine Geology 238, 93–106.
Paris, R., Wassmer, P., Sartohadi, J., Lavigne, F., Barthomeuf, B., Desgages, É., Grancher, D., Baumert, Ph., Vautier, F., Brunstein, D., Gomez, Ch., 2009. Tsunamis as geomorphic crisis: lessons from the December 26, 2004 tsunami in Lhok Nga, west Banda Aceh (Sumatra, Indonesia). Geomorphology 104, 59–72.
Paris, R., Cachao, M., Fournier, J., Voldoire, O., 2010. Nannoliths abundance and distribution in tsunami deposits: example from the December 26, 2004 tsunami Lhok Nga (northwest Sumatra, Indonesia). Géomorphologie: Relief, Processus, Environnement 1.
Pritchard, D., Dickinson, L., 2008. Modelling the sedimentary signature of long waves on coasts: implications for tsunami reconstruction. Sedimentary Geology 206, 42–57.
Scheffers, A., 2004. Tsunami imprints on the Leeward Netherlands Antilles (Aruba, Curaçao, Bonaire) and their relation to other coastal problems. Quaternary International 120, 163–172.
Shields, A., 1936. Application of similarity principles and turbulence research to bed-load movement. Mitteilunger der Preussischen Versuchsanstalt für Wasserbau und Schiffbau 26, 5–24.
Shiki, T., Yamazaki, T., 1996. Tsunami-induced conglomerates in Miocene upper bathyal deposits, Chita Peninsula, central Japan. Sedimentary Geology 104, 175–188.
Singarasubramanian, S.R., Mukesh, M.V., Manoharan, K., Murugan, S., Bakkairaj, D., Peter, A.J., 2006. Sediment characteristics of the M 9 tsunami event between Rameswaram and Thoothukudi, Gulf of Mannar, southeast coast of India. Science of Tsunami Hazards 25 (3), 160–172.
Soulsby, R.L., Whitehouse, R., 1997. Threshold of sediment motion in coastal environments. Proceedings of Pacific Coasts and Ports Conference 1. University of Canterbury, Christchurch, New Zealand, pp. 149–154.
Spiske, M., Böröcz, Z., Bahlburg, H., 2008. The role of porosity in discriminating between tsunami and hurricane emplacement of boulders — a case study from the Lesser Antilles, southern Caribbean. Earth and Planetary Science Letters 268, 384–396.
Srinivasalu, S., Thangadurai, N., Switzer, A.D., Ram Mohan, V., Ayyamperumal, T., 2007. Erosion and sedimentation in Kalpakkam (N Tamil Nadu, India) from the 26th December 2004 tsunami. Marine Geology 240, 65–75.
Szczucinski, W., Chaimanee, N., Niedzielski, P., Rachlewicz, G., Saisuttichai, D., Tepsuwan, T., Lorenc, S., Siepak, J., 2006. Environmental and geological impacts of the 26 December 2004 tsunami in coastal zone of Thailand — overview of short and long-term effects. Polish Journal of Environmental Studies 15 (5), 793–810.
Tanner, L.H., Calvari, S., 2004. Unusual sedimentary deposits on the SE side of Stromboli volcano, Italy: products of a tsunami caused by the ca. 5000 BP Sciarra del Fuoco collapse? Journal of Volcanology and Geothermal Research 137, 329–340.
Umitsu, M., Tanavud, C., Patanakanog, B., 2007. Effects of landforms on tsunami flow in the plains of Banda Aceh, Indonesia, and Nam Khem, Thailand. Marine Geology 242, 141–153.
Wassmer, P., Baumert, P., Lavigne, F., Paris, R., Sartohadi, J., 2007. Les transferts sédimentaires associés au tsunami du 26 décembre 2004 sur le littoral Est de Banda Aceh à Sumatra (Indonésie). Géomorphologie: Relief, Processus, Environnement 4, 335–346.
Weiss, R., 2008. Sediment grains moved by passing tsunami waves: tsunami deposits in deep water. Marine Geology 250 (3–4), 251–257.
Williams, D.M., Hall, A.M., 2004. Cliff-top megaclasts deposits of Ireland, a record of extreme waves in the North Atlantic — storms or tsunamis? Marine Geology 206, 101–117.
Yalin, M.S., 1972. Mechanics of Sediment Transport. Pergamon, New York.
Yawsangratt, S., Szczucinski, W., Chaimanee, N., Jagodzinski, R., Lorenc, S., Chatprasert, S., Saisuttichai, D., Tepsuwan, T., 2009. Depositional effects of 2004 tsunami and hypothetical paleotsunami near Thap Lamu Navy Base in Phang Nga Province, Thailand. Polish Journal of Environmental Studies 18 (1), 17–23.